Development 129, 1829-1838 (2002)
Printed in Great Britain © The Company of Biologists Limited 2002
DEV2839

Bile system morphogenesis defects and liver dysfunction upon targeted deletion of HNF1β

Catherine Coffinier[1,*,‡], Lionel Gresh[1,‡], Laurence Fiette[2], François Tronche[3,†], Günther Schütz[3], Charles Babinet[4], Marco Pontoglio[1], Moshe Yaniv[1,§] and Jacqueline Barra[4]

[1]Unité des Virus Oncogènes-CNRS URA 1644, Institut Pasteur, 25, rue du Docteur Roux, 75724 Paris Cedex 15, France
[2]Unité d'Expertise en Histotechnologie et Pathologie, Institut Pasteur, 25, rue du Docteur Roux, 75724 Paris Cedex 15, France
[3]Division Molecular Biology of the Cell I, DKFZ, Im Neuenheimer Feld 280, 69120 Heidelberg, Germany
[4]Unité de Biologie du Développement-CNRS URA 1960, Institut Pasteur, 25, rue du Docteur Roux, 75724 Paris Cedex 15, France
*Present address: Howard Hughes Medical Institute-UCLA, Los Angeles, CA 90095-1662, USA
†Present address: Institut de Biologie, CNRS FRE 2401, Collège de France, 11, place Marcelin Berthelot, 75231 Paris Cedex 5, France
‡Both authors contributed equally to this work
§Author for correspondence (e-mail: yaniv@pasteur.fr)

Accepted 21 January 2002

SUMMARY

The inactivation of the *Hnf1β* gene identified an essential role in epithelial differentiation of the visceral endoderm and resulted in early embryonic death. In the present study, we have specifically inactivated this gene in hepatocytes and bile duct cells using the Cre/loxP system. Mutant animals exhibited severe jaundice caused by abnormalities of the gallbladder and intrahepatic bile ducts (IHBD). The paucity of small IHBD was linked to a failure in the organization of duct structures during liver organogenesis, suggesting an essential function of *Hnf1b* in bile duct morphogenesis. Mutant mice also lacked interlobular arteries. As HNF1β is not expressed in these cells, it further emphasizes the link between arterial and biliary formation. Hepatocyte metabolism was also affected and we identified hepatocyte-specific HNF1β target genes involved in bile acids sensing and in fatty acid oxidation.

Key words: Cre/loxP, Bile duct, Epithelium differentiation, Gallbladder, Lipids

INTRODUCTION

Liver organogenesis starts around day 10 of mouse embryonic development and is completed after birth. This process requires the simultaneous differentiation of several cell types, including hepatocytes and biliary epithelial cells (BEC), and the formation of precise three-dimensional structures. Several groups have attempted to unravel the genetic program that controls hepatocytes and BEC differentiation by characterizing transcription factors enriched in these cells (Cereghini, 1996). Among these factors, the homeoprotein HNF1β/vHNF1 (hepatocyte nuclear factor 1β or variant hepatocyte nuclear factor 1) presents an interesting expression pattern. It is detectable in the hepatic bud and is abundantly expressed in the gallbladder primordium (Coffinier et al., 1999a). It is detected later in the intrahepatic bile ducts (IHBD) as they develop within the liver.

At the adult stage, HNF1β is strongly expressed throughout the biliary system. It is also expressed in periportal hepatocytes. This expression pattern distinguishes HNF1β from the closely related HNF1α protein that is uniformly distributed in all hepatocytes, and is expressed at lower levels in BEC (Pontoglio et al., 1996). The difference in expression of the two genes is interesting in light of the liver zonation phenomenon (Jungermann and Katz, 1982). Hepatocyte activities are specialized along the porto-central axis; catabolic metabolism occurs in the periportal hepatocytes, whereas anabolic functions are performed by hepatocytes closer to the central vein. Thus, the balance between the two HNF1 activities along the lobules may determine which hepatic genes are activated at a given position.

In addition to its hepatic expression, *Hnf1β* (Tcf2 – Mouse Genome Informatics) is strongly expressed in several epithelia organized in tubules, such as the pancreatic exocrine ducts and the kidney tubules (De Simone et al., 1991; Lazzaro et al., 1992). As HNF1β is expressed from the very onset of formation of such structures, it might play a role during differentiation and organogenesis (Coffinier et al., 1999a; Ott et al., 1991). Furthermore, gene inactivation demonstrated an early requirement for *Hnf1β* in the differentiation of another epithelium, the visceral endoderm (Barbacci et al., 1999; Coffinier et al., 1999b). HNF1β mutation blocks the differentiation of visceral endoderm and prevents its specialization into the two cell types that are specific for the embryonic and extra-embryonic territories. As visceral endoderm fails to differentiate, HNF1β-null mice die around the time of gastrulation, preventing further study of the role of HNF1β during later differentiation events.

To address the role of HNF1β in liver organogenesis, we generated a conditional allele of the gene and performed its tissue-specific inactivation in the liver using the Cre/loxP system (Gu et al., 1994). The loss of HNF1β in both hepatocytes and bile ducts resulted in a severe phenotype, including growth retardation and jaundice. Histological analysis of the gallbladder and the larger IHBD revealed epithelial abnormalities. We also observed a strong decrease in the number of the smaller IHBD and a persistence of the ductal plate from which IHBD are formed. These data suggest a requirement for HNF1β in biliary epithelium formation from the onset of the biliary system development. Biochemical and molecular studies of hepatic markers led to the identification of two HNF1β specific target genes, *Oatp1* (*Sla21a1* – Mouse Genome Informatics) and *Vlcad* (Acadvl – Mouse Genome Informatics), both of which are involved in lipid metabolism in hepatocytes.

MATERIALS AND METHODS

Gene targeting and conditional allele generation

A 5.8 kb genomic fragment containing the promoter and the first exon of *Hnf1β* was previously isolated from a mouse 129SVJ genomic library (Coffinier et al., 1999b). A conditional allele was generated by flanking the first exon with *loxP* sites for the Cre recombinase. A *loxP* site was inserted into a *Hin*cII site located 400 bp upstream of the transcription start site (Power and Cereghini, 1996) and a pgk-*neo* selection gene flanked by two additional *loxP* sites was introduced into a *Kpn*I site located 150 base pair downstream of the first exon. All three *loxP* sites were introduced in the same orientation as verified by sequencing. In addition, a pgk-*tk* gene isolated from pPNT was added downstream to the right recombination arm to allow double (Neo+ tk–) selection (Tybulewicz et al., 1991). CK35 ES cells (Kress et al., 1998) were electroporated with the linearized vector. After selection, G418-resistant clones genotype was probed by Southern blot analysis after *Xba*I digest using the two external probes previously described (Coffinier et al., 1999b), and five correctly recombined clones were identified. Cre-mediated recombination was obtained after electroporation of 10^7 recombinant ES cells using 15 μg pIC-Cre vector (Gu et al., 1993). After low-density plating, individual colonies were cultured in duplicate, in the presence or in absence of 300 μg/ml G418. After a 7-day culture, G418-sensitive clones were amplified and genotyped by PCR using primers flanking the *loxP* sites (*VHP9*, GGG GTG GCC TGC TCT AGG TGG C; *VHP8*, GCT CTC CAG GTC CTC CTC AGC TCC G; *VIR3*, CTT TTC GCT GCA CCC ACC AGC C; *EX11*, GTC CAA GCT CAC GTC GCT CC; *VIR4*, CCA GGT CTT TGC AGA GAA CTG C) (Fig. 1A). Out of 240 clones isolated after Cre expression, 50 had lost the selection gene, including 48 $Hnf1\beta^{del}$ and two $Hnf1\beta^{flox}$ clones, as identified by PCR. Both clones containing a floxed first exon and a deleted loci were isolated. Mice strains carrying either a $Hnf1\beta^{flox}$ or a $Hnf1\beta^{del}$ allele were established on a mixed C57BL/6 × 129SVJ background, and genotyped by PCR using the primers described above.

Liver-specific inactivation of the *Hnf1b* gene

The AlfpCre transgenic line (established on a FVB/N background) was used to produce HNF1β liver-specific inactivation (Kellendonk et al., 2000). β-galactosidase staining was performed according to standard procedures on animals resulting from the crossing of AlfpCre strain with the R26R strain (Soriano, 1999). Mice were genotyped using the primers described above and additional primers specific for the $Hnf1\beta^{lacZ}$ allele (Coffinier et al., 1999b) and the Cre transgene (Lakso et al., 1992). Cre recombination efficiency was assessed on liver DNA by Southern blot analysis after *Hin*dIII digest using a *Kpn*I-*Hin*dIII fragment located in the first intron as a probe. Control animals used in this study were of either $Hnf1\beta^{flox/+}$, $Hnf1\beta^{flox/+}$AlfpCre or $Hnf1\beta^{flox/lacZ}$. All animals were maintained under standard housing conditions.

Gene expression analysis

Northern blot analysis were performed on 30 μg of liver total RNA or 10 μg of kidney total RNA using *Hnf1β* and *Vlcad* cDNA probes, and a *Hprt* probe to normalize the samples. Expression of the differentiation markers were studied using semiquantitative RT-PCR as described previously (Coffinier et al., 1999b). The PCR cycle number were estimated for each primer pair to assure linear range amplification. The primer sequences are available on request.

Representational difference analysis of cDNA was carried out following a protocol supplied by M. Hubank (Hubank and Schatz, 1994). PolyA mRNA were purified from 2-week-old mutant and control liver total RNA (Dynabeads, Dynal). Double-stranded cDNA was prepared using oligo dT primer (Universal RiboClone cDNA Synthesis System, Promega).

Biochemical and histological analysis

Blood total and conjugated bilirubin concentrations were measured by colorimetry (Sigma – 552/553). After overnight fasting, blood triglycerides and cholesterol concentrations were measured enzymatically (Sigma – 336 and 352). Blood albumin and biliary acid concentrations were determined by Vebiotel laboratory (94110 Arcueil, France). Organs were fixed in formaldehyde 4% or Bouin's fixative, and embedded in paraffin using routine procedures. Sections (5 μm) were stained with Hematoxylin and Eosin.

Immunohistochemical procedure

Livers were frozen in isopentane cooled in a liquid nitrogen bath, and sectioned at 7 μm using a cryostat. Sections were air-dried overnight, fixed in acetone at 4°C for 10 minutes and washed in two changes of Tris-buffered saline and treated with a blocking buffer (TBS/normal goat serum 10%/bovine serum albumin 1%/Triton X-100 0.3%) for 30 minutes. Thereafter, sections were washed in TBS, incubated with primary antibody (rabbit anti-human keratin A0575, Dako or monoclonal anti-α smooth muscle actin 1A4, Dako; 1/250 dilution in TBS/normal goat serum 1%/BSA 0.1%/Triton X-100 0.3%) overnight at 4°C, washed again and incubated with secondary antibody (Envision+Peroxidase Rabbit, Dako or anti-mouse IgG, HRP-linked NA931, Amersham; 1/400 dilution) for 30-60 minutes at room temperature. Sections were stained with 3-amino-9-ethylcarbazole (ICN Biochemicals) and counterstained with Hematoxylin.

RESULTS

Generation of a HNF1β conditional allele

HNF1β null mutation resulted in an early embryonic lethality, owing to a defect in visceral endoderm differentiation (Barbacci et al., 1999; Coffinier et al., 1999b). We generated a conditional allele of the *Hnf1β* gene using the Cre/loxP system (Gu et al., 1994) to analyze potential functions at later stages of development. *loxP* sites for the Cre recombinase were introduced on both sides of the first exon followed by a PGK-neo selection marker also flanked by a *loxP* site (Fig. 1A). Removal of the *neo* selection cassette, by transient expression of the Cre should result in a conditional or floxed allele, as the remaining *loxP* should not interfere with gene expression (Fig. 1A). Recombination between the first and third *loxP* sites resulted in deletion of the first exon and creation of a null allele, $Hnf1\beta^{del}$. Two ES clones, one $Hnf1\beta^{del}$ and one $Hnf1\beta^{flox}$, were

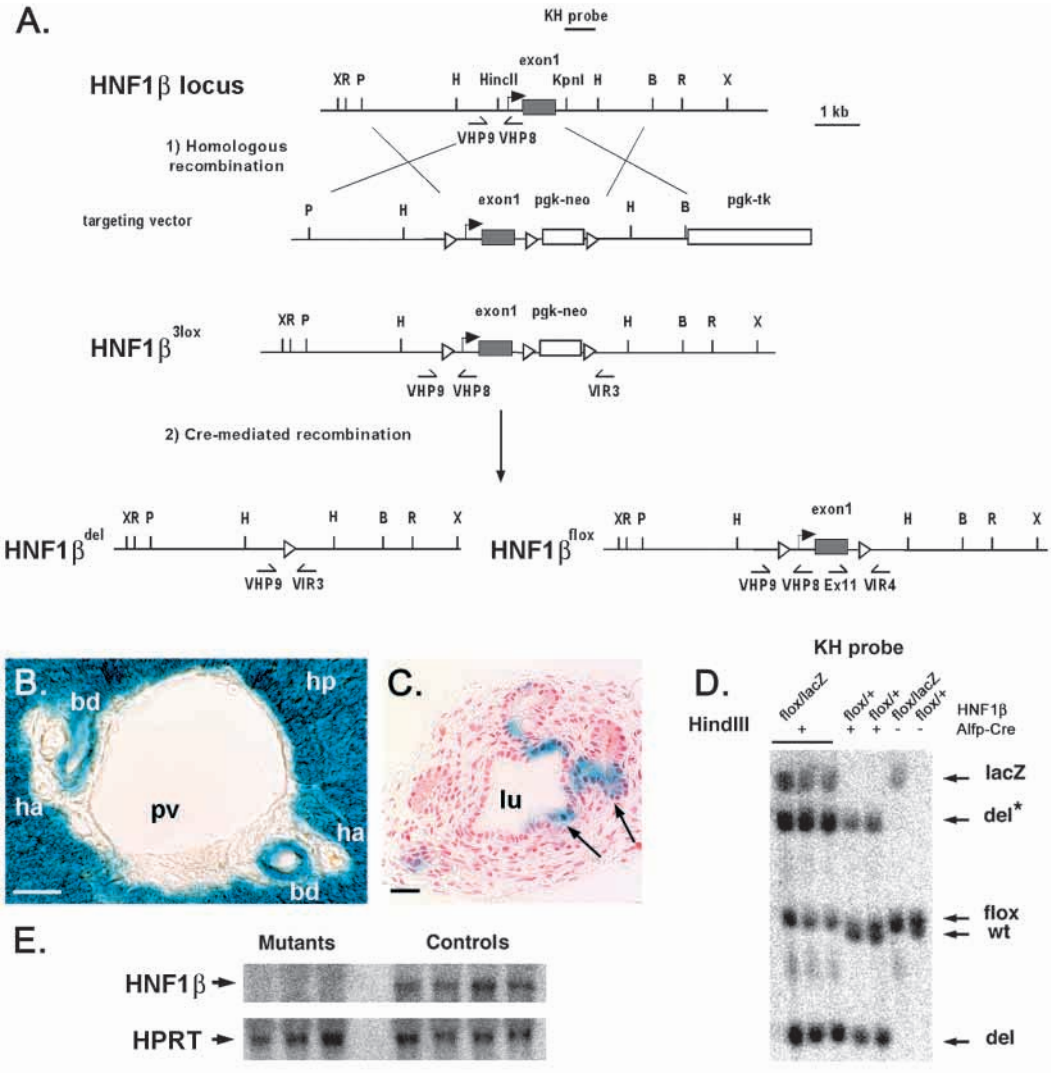

Fig. 1. Targeted inactivation of the *Hnf1β* gene in the liver. (A) Strategy used to generate the conditional allele, featuring the map of the murine locus, the recombinant allele $Hnf1\beta^{3lox}$ and the Cre-mediated alleles $Hnf1\beta^{flox}$ and $Hnf1\beta^{del}$. The DNA fragment used as probe for the genomic analysis is indicated as well as the primers used for genotyping. The first exon is featured by a gray box, the selection genes by white boxes, the *loxP* sites by triangles, and the promoter by an arrow. Restriction sites: Bm *Bam*HI; H, *Hin*dIII; P, *Pml*I; R, *Eco*RI; X, *Xba*I. (B,C) Cell specificity of Cre-mediated recombination in newborn AlfpCre; R26R mice. (B) β-galactosidase staining on vibratome section of liver, showing the specific activation of the *lacZ* transgene in the hepatic parenchyma (hp) and in the bile ducts (bd) but not in the wall of the portal vein (pv) and of the hepatic arterioles (ha). (C) Thin section through a gallbladder after β-galactosidase staining. Arrows indicate the staining of fields of the inner epithelium. lu, lumen. (D) Southern blot analysis of Cre-mediated recombination on liver DNA. Liver DNA from mice of either mutant ($Hnf1\beta^{lacZ/flox}$AlfpCre) or control genotypes ($Hnf1\beta^{flox/+}$, $Hnf1\beta^{flox/+}$AlfpCre or $Hnf1\beta^{flox/lacZ}$) were digested by the restriction enzyme *Hin*dIII and probed with the KH probe indicated on Fig. 1A. Bands characteristics for the different alleles are indicated on the right. Del* indicates a product of partial digestion specifically observed for the $Hnf1\beta^{del}$ allele. A rate of 80% conversion of the $Hnf1\beta^{flox}$ allele into the $Hnf1\beta^{del}$ form was estimated, by semi-quantitative PCR, for the Cre-positive animals. As hepatocytes represent about 70% of liver cells and biliary tree cells approximately 10%, we concluded that *Hnf1β* inactivation was achieved in a majority of hepatic cells. (E) Northern blot analysis of 1-month-old mutant and control liver RNA, showing the complete loss of HNF1β expression after Cre recombination. Total RNA was hybridized with HNF1β cDNA and after stripping probed for HPRT expression to check for loading. Scale bars: 100 μm.

injected into blastocysts to generate chimeric mice and heterozygous offspring. As previously reported, the $Hnf1\beta^{del/del}$ mutation resulted in an early embryonic lethality (Coffinier et al., 1999b). By contrast, $Hnf1\beta^{flox/flox}$ mice were born at a normal Mendelian ratio and were healthy and fertile. Thus, the $Hnf1\beta^{flox}$ allele is equivalent to a wild-type allele and deletion by the Cre recombinase should result into a null mutation, $Hnf1\beta^{del}$.

Liver-specific inactivation of the *Hnf1b* gene

In the liver, *Hnf1β* displays a complex expression pattern. It is strongly expressed in the biliary epithelial cells, and more weakly in the hepatocytes localized at the periphery of the hepatic lobules (Coffinier et al., 1999a). To inactivate the *Hnf1β* gene in both cell types, we required a Cre recombinase transgene expressed in these cells or in a common precursor. The *AlfpCre* transgene contains both albumin and α-fetoprotein regulatory elements, drives Cre recombinase expression in the hepatic bud as early as embryonic day 10 (E10) and targets both cell lineages (Kellendonk et al., 2000). To extend these initial data, AlfpCre activity was analyzed after crossing the AlfpCre transgenic mice with the ROSA26 Cre reporter line (R26R) carrying a *lacZ* gene that is activated after Cre-driven recombination (Soriano, 1999). Liver sections prepared at birth showed specific β-galactosidase staining in all hepatocytes and in all cells of the IHBD. By contrast no staining was detected in endothelial cells or portal vein mesenchyme (Fig. 1B). The homogenous staining suggested that efficient recombination occurred in both hepatocytes and biliary epithelial cells or more probably in the hepatoblast, the

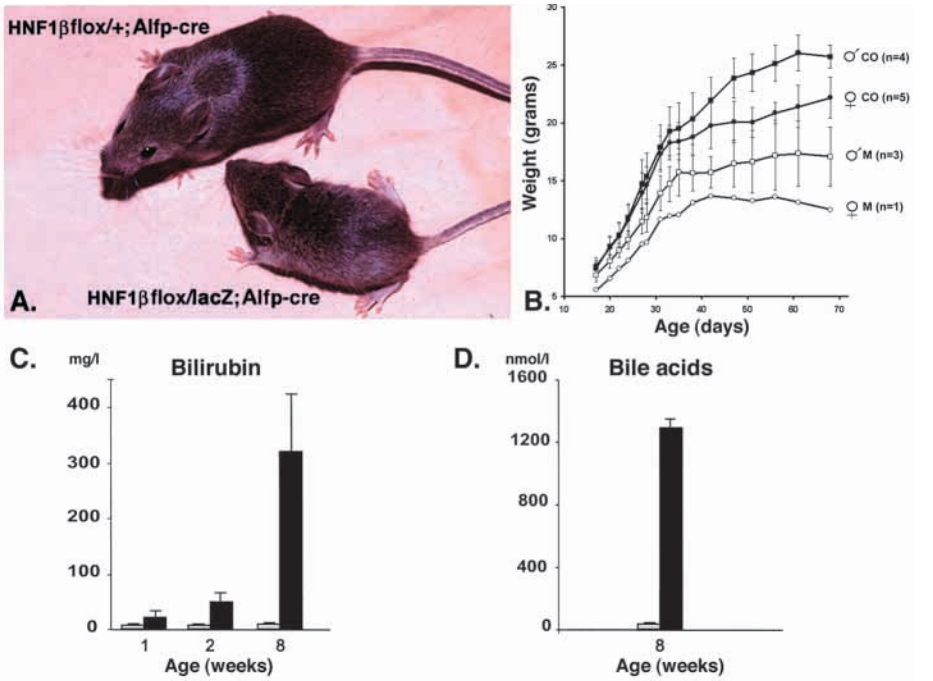

Fig. 2. HNF1β liver-specific mutation results in a severe growth defect and in accumulation of bile components in serum. (A) Picture of 2-month-old control and mutant littermates. (B) Growth curves of a litter resulting from a $Hnf1\beta^{flox/flox} \times Hnf1\beta^{lacZ/+}$AlfpCre cross. Weight was measured from day 15 after birth. Black squares, control (CO) males (mean of four mice); black circles, control females (mean of five mice); white squares, mutant (M) males (mean of three mice); white circles: a mutant female. Standard deviation for each sample is featured as error bars. (C,D) Biochemical analysis of bilirubin (C) and bile acids (D) levels in mutant (black bars) and control (gray bars) mice. Values are mean of 3-4 mice. All differences between mutant and controls were significant (P<0.05). Standard deviations for each sample are indicted by as error bars.

postulated common precursor of both cell types. Furthermore, these data confirm that Cre expression occurred before bile duct morphogenesis, which starts around E15, as differentiated biliary epithelial cells do not express the albumin gene (Shiojiri, 1997). In contrast to the uniform staining observed in the liver, the gallbladder sections showed only patches of β-galactosidase staining in the inner epithelium (Fig. 1C). As the gallbladder separates from the liver bud and stops expressing the albumin gene at day E10.5, the patchy staining suggests a shorter exposure to Cre activity, resulting in recombination events occurring only in a few precursor cells.

Liver-specific inactivation of the *Hnf1β* gene was achieved by crossing $Hnf1\beta^{flox/flox}$ mice with animals carrying one *Hnf1β* null allele and an AlfpCre transgene ($Hnf1\beta^{lacZ/+}$AlfpCre) (Coffinier et al., 1999b). One recombination event per cell was sufficient to generate a homozygous null mutation in $Hnf1\beta^{lacZ/flox}$AlfpCre offspring. Pups presenting the four possible genotypes were born in normal Mendelian ratios (data not shown). Recombination efficiency at the *Hnf1β* locus was confirmed by Southern blot analysis of liver DNA using a probe distinguishing between all four *Hnf1β* alleles: wild type, $Hnf1\beta^{lacZ}$, $Hnf1\beta^{flox}$ and $Hnf1\beta^{del}$ (Fig. 1D). To confirm the loss of *Hnf1β* expression in $Hnf1\beta^{lacZ/flox}$AlfpCre mice, a northern blot analysis was performed on total liver RNA using a probe specific for *Hnf1β* transcript. No *Hnf1β* RNA was detected in the mutant ($Hnf1\beta^{lacZ/+}$AlfpCre) livers compared with controls, either $Hnf1\beta^{flox/+}$, $Hnf1\beta^{flox/+}$AlfpCre or $Hnf1\beta^{flox/lacZ}$ (Fig. 1E). The loss of the transcript was tissue-specific as equal amounts of *Hnf1β* RNA were detected in total kidney RNA from both control and mutant animals (data not shown). Based on AlfpCre activity described above and on both DNA and RNA analysis, we concluded that Cre expression in the mutant mice led to the specific inactivation of the *Hnf1β* gene in hepatocytes and IHBD epithelial cells. In addition, our data suggested that partial deletion may have occurred in the gallbladder.

Hnf1β mutation results in severe growth retardation and jaundice

Liver-specific inactivation of the *Hnf1β* gene resulted in a clear phenotype. $Hnf1\beta^{lacZ/flox}$AlfpCre mice showed severe growth retardation, hypertrophy of the liver and chronic jaundice. Although some variations in the growth retardation were observed, the jaundice and the liver enlargement were fully penetrant among the mutant animals.

Body weight differences could be measured as early as day 2 after birth and increased with time (data not shown and Fig. 2A,B). The weight differences between mutant and control littermates were more dramatic by the time of weaning, reaching a growth plateau. In addition to their smaller size, mutants were cachectic with reduced adipose tissue and muscular atrophy. Despite the severity of their phenotype, most mutants survived for several months.

Jaundice, or high plasma levels of bilirubin, is a hallmark of hepatic or bile system damage. Bilirubin, an end metabolite of heme degradation, is formed in the liver and further processed into a conjugated form before secretion into the biliary system. Bilirubin conjugation is catalyzed in hepatocytes by uridine diphosphate glucuronosyltransferase (UGT). Accumulation of unconjugated bilirubin is an indicator of hepatic failure, whereas accumulation of conjugated bilirubin implies a post-hepatic defect, such as bile duct obstruction. Increased bilirubin levels were detectable 1 week after birth and reached 30-fold excess at 2 month stage (Fig. 2C). Despite this dramatic excess, conjugated bilirubin represented similar percentages of the total bilirubin in mutant and in control serum (mutants: 64.0±8.1%, n=5; controls: 71.5±10.2%, n=3). These results indicated a defect downstream of bilirubin processing. In addition, accumulation of conjugated bilirubin suggested that the conjugation machinery functions correctly in HNF1β mutant hepatocytes as a large excess of bilirubin was processed. Bile acids, other bile components generated by the catabolism of cholesterol, also showed a dramatic increase in adult serum (Fig. 2D).

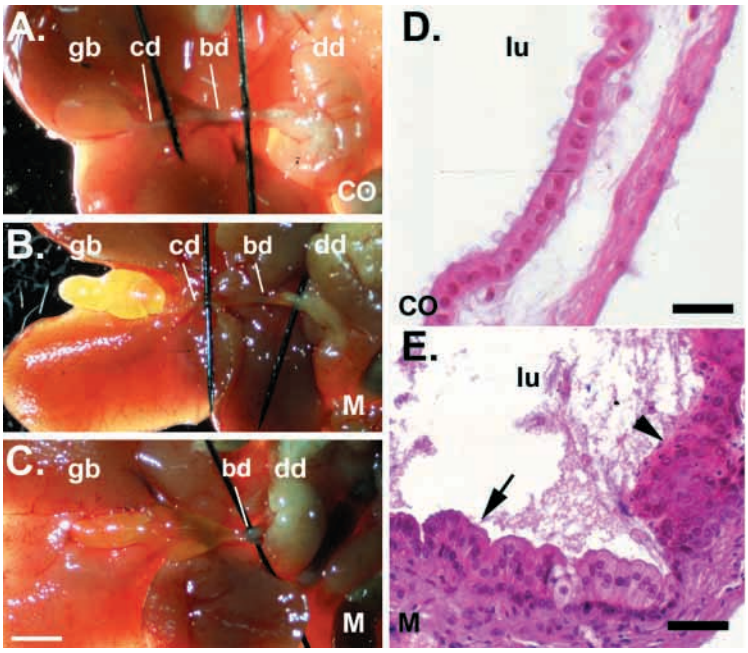

Fig. 3. Abnormal extrahepatic biliary epithelium in the mutant mice. (A-C) Extrahepatic biliary tract of 2-month-old control (A) and mutant (B,C) mice. Mutant gallbladders are irregularly shaped. Some mutants show dilated cystic duct. gb, gallbladder; cd, cystic duct; bd, common bile duct; dd, duodenum. Scale bars: 5mm. (D-E) Gallbladder sections for control (D) and mutant (E) animals. In the mutant sample, the normal cuboidal epithelium is replaced in some areas by a stratified squamous epithelium (arrowhead) or mucus-secreting cells (arrow). lu, lumen. Scale bars: 100 μm in D; 150 μm in E.

HNF1β mutation results in gallbladder epithelial dysplasia and in a paucity of intrahepatic bile ducts

Despite a probably incomplete deletion of the *Hnf1β* gene in the gallbladder, as suggested by the data reported in Fig. 1E, its morphology was strongly affected in mutant animals and was characterized by an irregular shape interrupted by several constrictions (Fig. 3A-C). In some extreme cases, the cystic duct was completely dilated and no duct was really identifiable; at the same time, the common bile duct was affected and the boundary between the two ducts could not be determined (Fig. 3C). Histological staining of tissue sections revealed that the inner layer of the gallbladder presented areas with disorganized epithelia in place of a typical cuboidal epithelium (Fig. 3D,E). Some of the abnormal cells presented a morphology reminiscent of mucus-secreting cells (Fig. 3E). Despite these abnormalities, the gallbladders were filled with bile and communicated normally with the liver and the duodenum. We conclude that extrahepatic biliary obstruction was not the cause of cholestasis.

Analysis of the IHBD revealed a dysplasia of the larger bile ducts and a reduced number, or paucity, of small IHBD. Immunostaining of liver sections with anti-cytokeratin (CK) antibodies specific for biliary cells (van Eyken et al., 1987) showed that, in two-month old mutant mice, most portal tracts did not contain any recognizable bile ducts (Fig. 4A,B). As this defect is already seen in 1-week-old mutant mice, it indicated the lack of formation of interlobular bile ducts. The larger bile ducts still present in mutant livers were abnormal. In contrast to normal bile ducts that are formed of a simple cuboidal epithelium, they were lined by a dysplasic multi-layered epithelium with delocalization of the nuclei from the basal membrane, both indicative of epithelial disorganization (Fig. 4C,D). These observations provide the first evidence that HNF1β participates in the genetic program that directs IHBD morphogenesis.

A lack of formation of interlobular arteries was also seen in mutant mice and confirmed by anti-α smooth muscle actin immunostaining (Fig. 5). As *Hnf1β* is not expressed in endothelial cells, this defect is probably a secondary consequence of the mutation. This observation points to a link between arterial and biliary development within the liver. As suggested by other groups, arteries-bile ducts interaction may play an important role in establishing three-dimensional liver structures during organogenesis (Desmet, 1992).

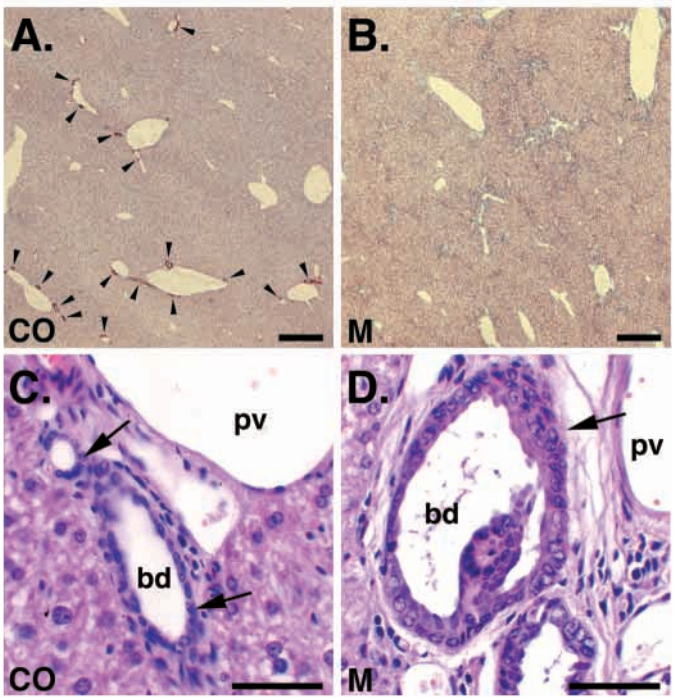

Fig. 4. Intrahepatic bile duct status in mutant mice.
(A,B) Immunostaining for cytokeratin (CK) on control (CO) and mutant (M) liver sections, isolated two months after birth.
(A) Control livers contain a large number of well differentiated bile ducts with a layer of CK-positive cells surrounding a lumen (arrowheads). (B) Mutant livers present a very disorganized biliary system. Most portal tracts do not contain any bile duct or CK-positive cell. Hepatocyte necrosis, inflammation and oval cell proliferation are also seen in mutant livers at this stage.
(C,D) Histological analysis of the larger intrahepatic bile ducts on control and mutant animals. Arrows in C indicate two normal bile ducts. The ducts of different size feature a single-layer epithelium with regularly spaced nuclei. By contrast, mutant bile ducts present a disorganized multi-layered epithelium (arrow in D). bd, bile duct; pv, portal vein. Scale bars: 1 mm in A,B; 100 μm in C,D.

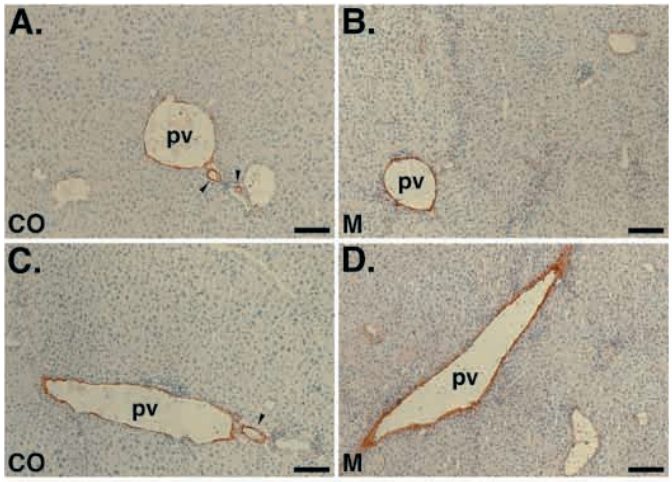

Fig. 5. Lack of arteries in mutant portal tracts. Immunostaining for α smooth muscle actin (SMA) on control (CO) and mutant (M) liver sections, isolated two months after birth. (A,C) Control livers show SMA-positive arteries (arrowheads) located around portal veins. Portal veins (pv) are also stained with the antibody. (B,D) In mutant livers almost all structures stained are veins. Only few large arteries are present. Scale bars: 100 μm.

HNF1β is essential for normal intrahepatic bile ducts differentiation and morphogenesis

To further analyze IHBD development in mutant mice, we stained liver sections at different stages with anti-cytokeratin (CK) antibodies. IHBD formation begins with the differentiation of hepatoblasts located at the interface between portal mesenchyme and liver parenchyma (Desmet and Callea, 1990). At E15.5, a continuous layer of CK-positive cells, also called ductal plate, is detected along the periportal mesenchyme. From E16.5 onwards, the bile ducts begin to differentiate by forming a lumen within the ductal plate that is surrounded by CK-positive cells (Fig. 6A,B). Bile duct differentiation progresses by the incorporation of the ducts within the periportal mesenchyme, while the ductal plate located between two adjacent bile duct regresses. By day 10 after birth (P10), bile duct differentiation is almost complete, although some remnant ductal plate can still be seen [see accompanying paper (Clotman et al., 2002) and Fig. 6E]. In contrast to the pattern observed for the control animals, E17.5 mutant embryos showed a very disorganized ductal plate with irregular lumens and the layer of CK-positive cells surrounding lumens displayed interruptions (Fig. 6C,D).

IHBD developmental defects resulted in a very disorganized biliary system. For each mutant animal (n=4), less than 5% of the portal tracts presented a normal duct pattern at day 8. 42±4% of the portal tracts lacked any bile duct-like cells or showed few CK-positive remaining from the ductal plate (Fig. 6F). By contrast, 46±9% of portal tracts presented strong CK staining, either as remnants of the ductal plate or as clusters of CK-positive cells incorporated in the portal mesenchyme but lacking a normal lumen (Fig. 6G). In some cases, dysplasic bile ducts were also observed (Fig. 6H). In conclusion, cell-specific *Hnf1β* deletion led to important morphogenetic defects of the developing IHBD. The paucity of IHBD observed postnatally in the biliary tract is probably caused by a failure to organize normal ducts. Therefore HNF1β plays an essential role in the differentiation of the IHBD.

Hnf1β is required for lipid metabolism

To further probe the consequence of HNF1β inactivation in the liver, a panel of biochemical parameters was analyzed in the serum of both mutant and control littermates. General hepatic functions were assessed by measuring the level of serum albumin. No significant difference was detected between the mutants (22.2±2.9 g/l; n=4) and controls (25.7±3.1 g/l; n=4). However, in addition to the accumulation of bilirubin and bile acids described above, the levels of serum cholesterol and triglycerides were found to be dramatically increased, as early as one week after birth (Fig. 7A,B). These levels increased between 1 and 2 weeks of age and then became stabilized. Bile represents a major route for the excretion of organic solutes, such as bilirubin. Furthermore, cholesterol degradation into bile acids and biliary cholesterol secretion are the major pathways to eliminate excess cholesterol (Repa and Mangelsdorf, 2000). Thus, bilirubin, bile acids and cholesterol accumulation observed in mutant mice could result from a reduced bile flow due to IHBD paucity. These accumulations could also be due to the combined effect of a hepatocytic defect and a bile flow defect. Indeed, high levels of triglycerides suggested that hepatocyte metabolism may be affected by *Hnf1β* liver-specific deletion.

The loss of HNF1β affects the expression of hepatocyte-specific genes

To characterize the hepatocyte defects and to identify liver-specific HNF1β target genes, we analyzed the expression of a number of hepatic genes by RT-PCR on total liver RNA. The expression of the liver-enriched transcription factors, *Hnf1α* (*Tcf1* – Mouse Genome Informatics), *Hnf4α*, *Hnf3β* (*Foxa2* – Mouse Genome Informatics) and *Hnf6* (*Onecut1* – Mouse Genome Informatics) was not significantly affected by the loss of HNF1β (data not shown). The expression of the secreted protein Transthyretin, the epithelial marker E-cadherin and the hepatocyte-specific connexin 32 were also normal (data not shown). As lipid metabolism was strongly perturbed in the mutants, we studied the expression of the apolipoproteins AI, AII, AIV, B, CII, CIII and E, which were all expressed at similar levels between mutants and controls (data not shown). We also examined the expression levels of molecules involved in bile formation. For example, bile acids are produced in the liver from cholesterol through two alternative pathways (Russell and Setchell, 1992). The cholesterol hydroxylase Cyp7α performs the first step of the major pathway, whereas it is carried out by Cyp27 in the alternative pathway. Both *Cyp7a* and *Cyp27* were normally expressed in the mutant livers compared with controls (data not shown). Recent studies have demonstrated that biliary acid synthesis is tightly regulated by transcription factors of the nuclear receptor family. LXRα stimulates Cyp7α expression after binding to oxysterols (Janowski et al., 1996), whereas FXR, SHP-1 and LRH-1 participate in a negative feedback loop activated by bile acids (Goodwin et al., 2000; Lu et al., 2000). Surprisingly, despite the huge excess of bile acids accumulated in the mutant tissues, no variation was observed in the expression of these nuclear receptors between mutants and controls (data not shown).

Bile traffic involves numerous transporters (Kullak-Ublick

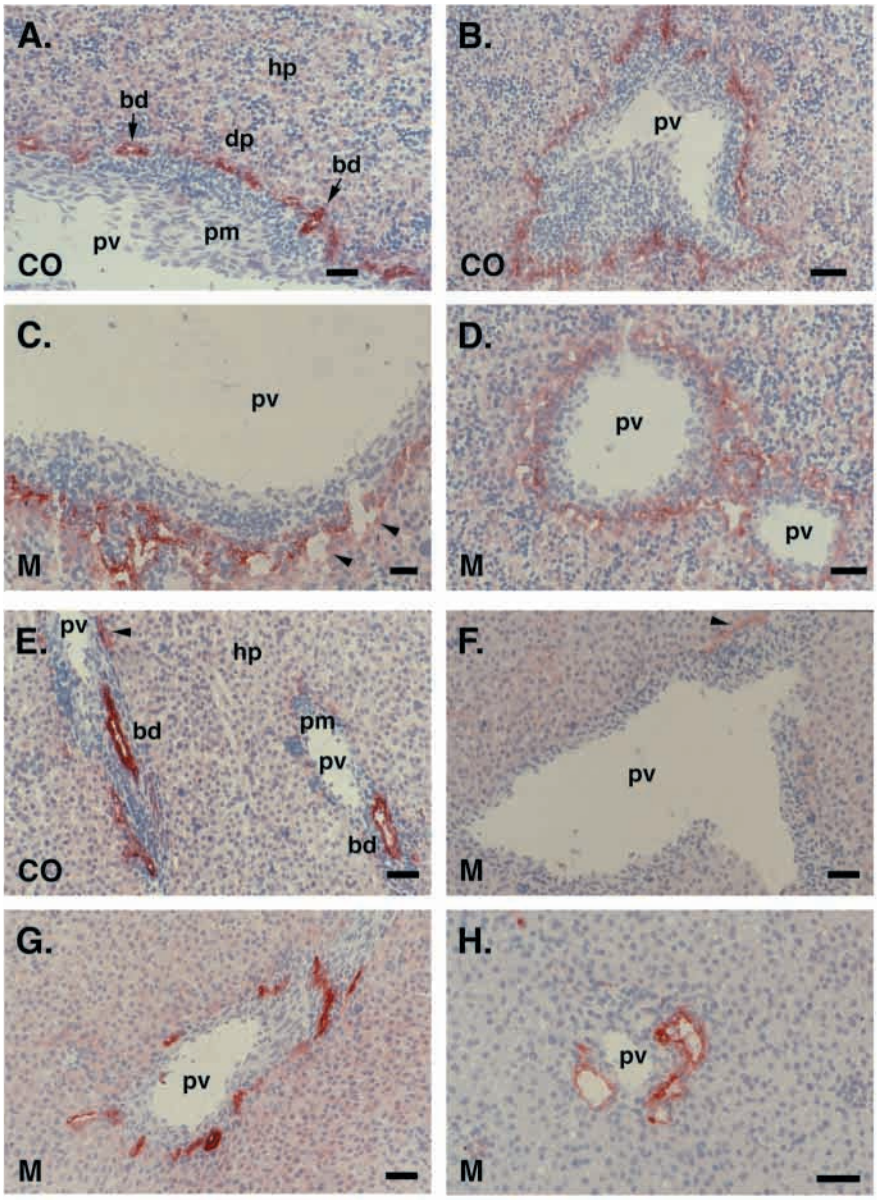

Fig. 6. The *Hnf1β* mutation affects intrahepatic bile duct development. Immunostaining for cytokeratin (CK) on control (CO) and mutant (M) liver sections. (A-D) E17.5 fetuses. (A,B) Control livers show a well-formed and stained ductal plate, and some bile ducts that are beginning to differentiate (arrows). (C,D) Mutant livers show disorganized ductal plate with irregular duct-like structures not completely surrounded by CK-positive cells (arrowheads). (E-H) P8 livers. (E) Differentiated bile ducts are seen on control mice. Some remnants of the ductal plate are still visible (arrowhead). (F-H) Mutants show no or very few CK-positive cells (arrowhead) (F), ductal plate remnants and abnormal CK-positive structures within the portal mesenchyme (G), or abnormal bile ducts (H). hp, hepatic parenchyma; pv, portal vein; pm, portal mesenchyme; dp, ductal plate; bd, bile ducts. Scale bars: 50 μm.

et al., 2000; Trauner et al., 1998). Ntcp (Slc10a1), a Na^+-dependent transporter, and the sodium independent transporters, Oatp1, Oatp2 and Oatp4 (Slc21a1, Slc21a5 and Slc21a6), participate in the reabsorption of bile acids from the blood in the sinusoids toward the hepatocytes. They play an important role in allowing the sensing of bile acid levels in the blood by hepatocytes. cMoat (canalicular multiple organic anion transporter; Abcc2 – Mouse Genome Informatics) and Bsep (bile salt export pump; Abcb11 – Mouse Genome Informatics) deliver, respectively, bilirubin and bile acids from the hepatocytes to the bile ductule. We found that *Oatp1* was specifically downregulated in the absence of HNF1β, whereas the other six transporters remained almost unaffected (Fig. 7C and data not shown). This decrease in *Oatp1* expression was observed in 2-week-old mice, suggesting that it could be a direct consequence of HNF1β deletion in hepatocytes and not a secondary effect of cholestasis. Interestingly, Oatp1 is also a target of HNF1α factor (Shih et al., 2001). Oatp1 downregulation could also contribute to the bile acid accumulation in the serum, as bile acids will then be less efficiently reabsorbed from blood.

Data resulting from the use of representational difference analysis (RDA) of cDNA (Hubank and Schatz, 1994) of mutant versus control livers led to the identification of another HNF1β target gene. The transcription of very long chain acetylCoA dehydrogenase (*Vlcad*), one of the four key enzymes of fatty acid oxidation (Beinert, 1963), was strongly decreased in the mutant samples (Fig. 7D). The *Vlcad* promoter (GenBank Accession Number, AJ012054) contains two HNF1 consensus binding sites located at positions –71 and –332, but its expression is not affected in the *Hnf1α*$^{-/-}$ mice (data not shown). Therefore, VLCAD constitutes a HNF1β specific target gene. A defect in fatty acid oxidation could account for the accumulation of triglycerides observed in the mutant serums. As fatty acid oxidation is performed by hepatocytes, this further indicates that HNF1β plays specific roles in hepatocyte functions.

DISCUSSION

The liver fulfills many essential functions in mammalian organisms. The organ is formed from several cell types that are organized into a well defined three-dimensional structure. HNF1α and HNF1β were initially characterized as two closely related homeoproteins that activate the transcription of liver-specific genes. Subsequent studies showed that both proteins have a more extended expression pattern, including epithelial cells of the kidney, pancreas and intestine (Blumenfeld et al., 1991; Coffinier et al., 1999a; De Simone et al., 1991; Lazzaro et al., 1992; Pontoglio et al., 1996). *Hnf1α* is not essential for normal mouse development, but its absence results in hepatic, pancreatic and renal functional defects (Pontoglio et al., 1996;

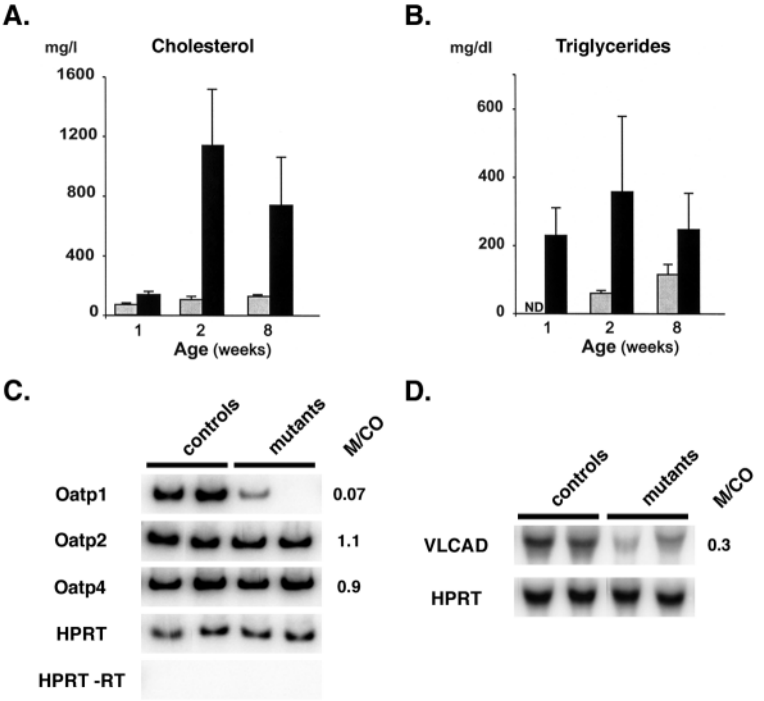

Fig. 7. (A,B) HNF1β is required for the general lipid homeostasis. Biochemical analysis of cholesterol (A) and triglycerides (B) levels in mutant (black bars) and control (gray bars) mice at the age of 1 week (n=8), 2 weeks (n=6) and 8 weeks (n=6). All differences between mutant and controls were significant (P<0.05). There is no significant difference between 2- and 8-week-old mutants. Triglyceride level for 1-week-old mutant is abnormally elevated despite the lack of comparison with the control. Standard deviation for each sample is featured as error bars. (C,D) HNF1β is required for the expression of the Oatp1 transporter and the fatty acid dehydrogenase VLCAD. (C) Semi-quantitative RT-PCR analysis of liver organic anion transporters expression (Slc21a1/Oatp1; Slc21a5/Oatp2; Slc21a6/Oatp4). Genotypes are indicated on top. HPRT primers were used as a normalizing standard for the RT samples (HPRT) and as a reverse transcription control (HPRT –RT). Gene expression was measured in six mice for each genotype. (D) Northern blot analysis of very long chain acetylCoA dehydrogenase (VLCAD) mRNA levels. HPRT cDNA probe is used as a normalizing standard. Gene expression was measured in four mice for each genotype. Ratios between mutants and controls are shown after HPRT normalization (M/CO).

Pontoglio et al., 1998; Pontoglio et al., 2000; Shih et al., 2001). By contrast, *Hnf1β* is required for early mouse development. In particular, it is essential for the proper differentiation of the visceral endoderm during gastrulation (Barbacci et al., 1999; Coffinier et al., 1999b). In the present study we investigated the potential role played by HNF1β during development and organogenesis using cell-specific gene inactivation. We demonstrate that HNF1β is essential for the formation of a functional bile duct system and for several hepatic metabolic functions.

Replacement of the first exon of HNF1β with β-galactosidase followed by in situ staining has demonstrated that this gene is abundantly transcribed in the bile duct epithelium (Coffinier et al., 1999a). Much lower expression was observed in periportal hepatocytes. To inactivate the gene in both cell types, we crossed HNF1β floxed mice with an AlfpCre mouse. This mouse was shown to express the recombinase in the liver primordium from day 10 of gestation. At this time point, the Cre should be expressed in the hepatoblast that give rise to both hepatocytes and biliary duct cells. Crosses between the AlfpCre mouse and the ROSA26 floxed β-galactosidase reporter strain, showed that inactivation occurred in both cell types. Furthermore we have seen that partial inactivation occurs in the gallbladder epithelium.

HNF1β is an essential factor in the intrahepatic bile duct differentiation pathway

Inactivation of HNF1β in precursors of intrahepatic biliary epithelium led to paucity of interlobular bile ducts and dysplasia of larger hepatic bile ducts epithelia. Immunohistochemical analysis showed that bile duct defects were already present at E17.5, and that ductal plate, from which IHBD develop, abnormally persisted after birth in mutant mice. Paucity of IHBD is thus directly linked to a developmental defect, demonstrating that HNF1β is essential for normal IHBD morphogenesis during liver formation. Similar features were observed in *Hnf6*$^{-/-}$ mice, demonstrating that both HNF1β and HNF6 act in a transcription factor network involved in IHBD formation [see accompanying paper (Clotman et al., 2002)]. The results from Clotman et al., suggest that a HNF6→HNF1β cascade may be an important component of this network. These two complementary studies are the first to identify specific transcription factors involved in the IHBD differentiation program. In addition to the paucity of small IHBD observed in newborn, we observed a dysplasia of larger IHBD and of the gallbladder. The epithelium presented abnormal characteristics with a delocalization of the nuclei from the base of the cell, the organization of multiple layers of cells or the presence of ectopic epithelium. These observations suggest an effect of *Hnf1β* inactivation on the maintenance of epithelial differentiation. As previously suggested for the visceral endoderm, HNF1β could regulate fundamental characters of epithelium identity such as the basal position of the nuclei and the growth in monolayer of cells. Thus, HNF1β seems to have a dual function in controlling both the differentiation and the proliferation of certain epithelial cells.

Paucity of IHBD correlates, in mutant mice, with a lack of interlobular arteries. As *Hnf1β* is not expressed in endothelial cells, this defect is an indirect consequence of the mutation. These findings demonstrate that proper morphogenesis of bile ducts is necessary for arterial vascularization of the liver. Intercellular signals from biliary epithelial cells may act on endothelial or smooth muscle cells differentiation and/or proliferation to establish the correct three-dimensional liver organization.

Relationship with human diseases

Human autosomal dominant mutations in the *Hnf1β* gene result in a particular form of type II diabetes called maturity onset diabetes of the young type 5 (MODY5) (Horikawa et al., 1997).

In some of the carriers of these mutations, kidney developmental defects, which are associated with internal genital abnormalities, were also observed (Lindner et al., 1999; Nishigori et al., 1998). Liver function of individuals with MODY5 was poorly investigated, owing to the low occurrence of cases. However, a liver function exploration in Japanese individuals with MODY5 reported high levels of γ-glutamyl transpeptidase, aspartate and alanine amino transferases, indicative of hepatic failure (Iwasaki et al., 1998). A case of hyperbilirubinemia was also described. These values were significantly higher than normal values and were not observed in individuals with MODY1/HNF4α or MODY3/HNF1α, suggesting that autosomal dominant HNF1β mutations may, at least in some cases, be specifically associated with liver dysfunction. Whether this liver dysfunction is linked to bile duct defects similar to those observed in mice, remains unknown.

Congenital diseases of IHBD can affect different levels of the biliary tree and can be characterized by dilatation or involution of the bile duct structures. All these diseases seem to have a developmental origin and to result from ductal plate remodeling problems, also called 'ductal plate malformations' (DPM) (Desmet, 1992). The hepatic phenotype of HNF1β-liver specific inactivation mice resembles, in some aspects, two human syndromes: Alagille's syndrome, which is characterized by a paucity of interlobular bile ducts, and Caroli's disease, a congenital non-obstructive dilatation of the larger IHBD. However, the phenotype of our mutant mouse does not perfectly match the description of these congenital diseases. Despite the divergence of phenotypes observed, study of mice lacking *Hnf1β* may provide some insights into the early development of DPM disease in humans.

HNF1α/HNF1β duality and hepatic functions

Hnf1α and *Hnf1β* were initially characterized as liver-specific genes participating in a network of transcription factors. In vitro studies showed that both proteins bind the same DNA sequences with similar affinities. It has led to a model proposing that the balance between the strong transactivator HNF1α and the weaker HNF1β constitutes a major element in HNF1 target gene regulation (Baumhueter et al., 1988; Rey-Campos et al., 1991; Song et al., 1998). However, studies of knockout mice have revealed that the molecular basis for this regulation might be more complex. For example, in the *Hnf1α*$^{-/-}$ mutants, the expression of several renal transporters were strongly affected despite the presence of large amounts of HNF1β in the same renal cells (Pontoglio et al., 2000), suggesting that HNF1α possesses distinct functions. We present evidence that in hepatocytes, despite the presence of large excess of HNF1α protein, HNF1β is necessary for activation specific target genes as shown by the decreased transcription of hepatic transporter *Oatp1* and *Vlcad* enzyme in the mutant livers.

Oatp1 participates in the reabsorption of bile acids from the blood. *Oatp1* loss of expression could contribute to the accumulation of bile acids in the blood. As *Oatp1* is also a target of HNF1α (Shih et al., 2001), this gene may depend upon transactivation by HNF1α/HNF1β heterodimers. By contrast, VLCAD, a key enzyme of fatty acid oxidation, is affected by *Hnf1β* mutation but not by *Hnf1α* mutation, suggesting a requirement for HNF1β homodimers.

In conclusion, our results show that in hepatocytes HNF1β has a specific role not fully redundant with HNF1α. Moreover, metabolic abnormalities observed in the mutants correlate strikingly with the expression of the *Hnf1β* gene in the liver. Owing to the functional zonation of hepatocytes in the lobules, the periportal hepatocytes are the major site of bile excretion and of oxidative energetic metabolism, including fatty acid oxidation (Jungermann and Katz, 1982). As reported in a previous study, HNF1β is expressed in a subpopulation of hepatocytes located at the lobule periphery, whereas HNF1α has been shown to be expressed in all hepatocytes (Coffinier et al., 1999a; Pontoglio et al., 1996). Thus, only the periportal hepatocytes would be affected by the loss of HNF1β, which correlates with the alterations of biliary acids transport and fatty acid oxidation. We propose that the abnormal HNF1 activity in this subpopulation of cells, which is due to the lack of HNF1β, resulted in a strong decrease of Oatp1 and VLCAD expression. These observations indicate that HNF1β may participate to establish functional zonation within the liver by specification of periportal hepatocytes.

Finally, HNF1β is also expressed in other tubular structures such as pancreatic exocrine ducts and kidney tubules (Coffinier et al., 1999a). Moreover, this expression starts with the onset of differentiation of these structures. The role of HNF1β in bile duct formation and its specific expression pattern suggests that this gene could also be controlling pancreatic ducts and kidney tubule morphogenesis. HNF1β could be part of a general developmental program leading to establishment of epithelial tubular structures during organogenesis of several organs. This question may be addressed by studying crosses of the *Hnf1β* floxed mouse with other cell-specific Cre-expressing mice.

We are grateful to F. Lemaigre and his team for sharing results before publication. We thank M. Hadchouel and G. Kullak-Ublick for helpful discussion, P. Soriano for the ROSA26R mouse strain, H. Khun, S. Garbay, A. Doyen, P. Ave, J.-C. Benichou and J.-P. Bourgeois for advice, and C. Médaille from Vebiotel (Arcueil, France) for blood albumin and biliary acids measurement. We are grateful to J. Weitzman for critical reading of the manuscript. C. C. was a recipient of a fellowship of the Foundation Roux. L. G. was supported by a fellowship from the French ministry of Education and Research. M. Y. thanks the Kougie & Bert Vallee Foundation for support.

REFERENCES

Barbacci, E., Reber, M., Ott, M. O., Breillat, C., Huetz, F. and Cereghini, S. (1999). Variant hepatocyte nuclear factor 1 is required for visceral endoderm specification. *Development* **126**, 4795-4805.

Baumhueter, S., Courtois, G. and Crabtree, G. R. (1988). A variant nuclear protein in dedifferentiated hepatoma cells binds to the same functional sequences in the beta fibrinogen gene promoter as HNF-1. *EMBO J.* **7**, 2485-2493.

Beinert, N. (1963). Acyl-CoA dehydrogenases. In *The Enzymes*, Vol. 7 (ed. P. D. Boyer, H. Lardy and K. Myrback), pp. 447-476. New York, NY: Academic Press.

Blumenfeld, M., Maury, M., Chouard, T., Yaniv, M. and Condamine, H. (1991). Hepatic nuclear factor 1 (HNF1) shows a wider distribution than products of its known target genes in developing mouse. *Development* **113**, 589-599.

Cereghini, S. (1996). Liver-enriched transcription factors and hepatocyte differentiation. *FASEB J.* **10**, 267-282.

Clotman, F., Lannoy, V. J., Reber, M., Cereghini, S., Cassiman, D., Jacquemin, P., Roskams, T., Rousseau, G. G. and Lemaigre, F. P. (2002).

The onecut transcription factor HNF6 is required for normal development of the biliary tract. *Development* **129**, 1819-1828.

Coffinier, C., Barra, J., Babinet, C. and Yaniv, M. (1999a). Expression of the vHNF1/HNF1beta homeoprotein gene during mouse organogenesis. *Mech. Dev.* **89**, 211-213.

Coffinier, C., Thepot, D., Babinet, C., Yaniv, M. and Barra, J. (1999b). Essential role for the homeoprotein vHNF1/HNF1beta in visceral endoderm differentiation. *Development* **126**, 4785-4794.

De Simone, V., De Magistris, L., Lazzaro, D., Gerstner, J., Monaci, P., Nicosia, A. and Cortese, R. (1991). LFB3, a heterodimer-forming homeoprotein of the LFB1 family, is expressed in specialized epithelia. *EMBO J.* **10**, 1435-1443.

Desmet, V. J. (1992). Congenital diseases of intrahepatic bile ducts: variations on the theme 'ductal plate malformation'. *Hepatology* **16**, 1069-1083.

Desmet, V. J. and Callea, F. (1990). Cholestatic syndromes of infancy and childhood. In *Hepatology. A Text Book for Liver Disease* (ed. D. Zakim and T. D. Boyer), pp. 1355-1395. London: Saunder.

Goodwin, B., Jones, S. A., Price, R. R., Watson, M. A., McKee, D. D., Moore, L. B., Galardi, C., Wilson, J. G., Lewis, M. C., Roth, M. E. et al. (2000). A regulatory cascade of the nuclear receptors FXR, SHP-1, and LRH-1 represses bile acid biosynthesis. *Mol. Cell* **6**, 517-526.

Gu, H., Zhou, Y. R. and Rajewsky, K. (1993). Independent control of immunoglobulin switch at individual switch regions evidenced through the Cre-loxP-mediated gene targeting. *Cell* **73**, 1155-1164.

Gu, H., Marth, J. D., Orban, P. C., Mossmann, H. and Rajewsky, K. (1994). Deletion of a DNA polymerase beta gene segment in T cells using cell type-specific gene targeting. *Science* **265**, 103-106.

Horikawa, Y., Iwasaki, N., Hara, M., Furuta, H., Hinokio, Y., Cockburn, B. N., Lindner, T., Yamagata, K., Ogata, M., Tomonaga, O. et al. (1997). Mutation in hepatocyte nuclear factor-1 beta gene (TCF2) associated with MODY. *Nat. Genet.* **17**, 384-385.

Hubank, M. and Schatz, D. G. (1994). Identifying differences in mRNA expression by representational difference analysis of cDNA. *Nucleic Acids Res.* **22**, 5640-5648.

Iwasaki, N., Ogata, M., Tomonaga, O., Kuroki, H., Kasahara, T., Yano, N. and Iwamoto, Y. (1998). Liver and kidney function in Japanese patients with maturity-onset diabetes of the young. *Diabetes Care* **21**, 2144-2148.

Janowski, B. A., Willy, P. J., Devi, T. R., Falck, J. R. and Mangelsdorf, D. J. (1996). An oxysterol signalling pathway mediated by the nuclear receptor LXRalpha. *Nature* **383**, 728-731.

Jungermann, K. and Katz, N. (1982). Functional hepatocellular heterogeneity. *Hepatology* **2**, 385-395.

Kellendonk, C., Opherk, C., Anlag, K., Schutz, G. and Tronche, F. (2000). Hepatocyte-specific expression of Cre recombinase. *Genesis* **26**, 151-153.

Kress, C., Vandormael-Pournin, S., Baldacci, P., Cohen-Tannoudji, M. and Babinet, C. (1998). Nonpermissiveness for mouse embryonic stem (ES) cell derivation circumvented by a single backcross to 129/Sv strain: establishment of ES cell lines bearing the *Om*^{d} conditional lethal mutation. *Mamm. Genome* **9**, 998-1001.

Kullak-Ublick, G. A., Stieger, B., Hagenbuch, B. and Meier, P. J. (2000). Hepatic transport of bile salts. *Semin Liver Dis.* **20**, 273-292.

Lakso, M., Sauer, B., Mosinger, B. J., Lee, E. J., Manning, R. W., Yu, S. H., Mulder, K. L. and Westphal, H. (1992). Targeted oncogene activation by site-specific recombination in transgenic mice. *Proc. Natl. Acad. Sci. USA* **89**, 6232-6236.

Lazzaro, D., De Simone, V., De Magistris, L., Lehtonen, E. and Cortese, R. (1992). LFB1 and LFB3 homeoproteins are sequentially expressed during kidney development. *Development* **114**, 469-479.

Lindner, T. H., Njolstad, P. R., Horikawa, Y., Bostad, L., Bell, G. I. and Sovik, O. (1999). A novel syndrome of diabetes mellitus, renal dysfunction and genital malformation associated with a partial deletion of the pseudo-POU domain of hepatocyte nuclear factor-1beta. *Hum. Mol. Genet.* **8**, 2001-2008.

Lu, T. T., Makishima, M., Repa, J. J., Schoonjans, K., Kerr, T. A., Auwerx, J. and Mangelsdorf, D. J. (2000). Molecular basis for feedback regulation of bile acid synthesis by nuclear receptors. *Mol. Cell* **6**, 507-515.

Nishigori, H., Yamada, S., Kohama, T., Tomura, H., Sho, K., Horikawa, Y., Bell, G. I., Takeuchi, T. and Takeda, J. (1998). Frameshift mutation, A263fsinsGG, in the hepatocyte nuclear factor-1beta gene associated with diabetes and renal dysfunction. *Diabetes* **47**, 1354-1355.

Ott, M. O., Rey-Campos, J., Cereghini, S. and Yaniv, M. (1991). vHNF1 is expressed in epithelial cells of distinct embryonic origin during development and precedes HNF1 expression. *Mech. Dev.* **36**, 47-58.

Pontoglio, M., Barra, J., Hadchouel, M., Doyen, A., Kress, C., Bach, J. P., Babinet, C. and Yaniv, M. (1996). Hepatocyte nuclear factor 1 inactivation results in hepatic dysfunction, phenylketonuria, and renal Fanconi syndrome. *Cell* **84**, 575-585.

Pontoglio, M., Prié, D., Cheret, C., Doyen, A., Leroy, C., Froguel, P., Velho, G., Yaniv, Y. and Friedlander, G. (2000). HNF1 controls renal glucose reabsorption in mouse and man. *EMBO Rep.* **1**, 359-365.

Pontoglio, M., Sreenan, S., Roe, M., Pugh, W., Ostrega, D., Doyen, A., Pick, A. J., Baldwin, A., Velho, G., Froguel, P. et al. (1998). Defective insulin secretion in hepatocyte nuclear factor 1alpha- deficient mice. *J. Clin. Invest.* **101**, 2215-2222.

Power, S. C. and Cereghini, S. (1996). Positive regulation of the vHNF1 promoter by the orphan receptors COUP-TF1/Ear3 and COUP-TFII/Arp1. *Mol. Cell. Biol.* **16**, 778-791.

Repa, J. J. and Mangelsdorf, D. J. (2000). The role of orphan nuclear receptors in the regulation of cholesterol homeostasis. *Annu. Rev. Cell Dev. Biol.* **16**, 459-481.

Rey-Campos, J., Chouard, T., Yaniv, M. and Cereghini, S. (1991). vHNF1 is a homeoprotein that activates transcription and forms heterodimers with HNF1. *EMBO J.* **10**, 1445-1457.

Russell, D. W. and Setchell, K. D. (1992). Bile acid biosynthesis. *Biochemistry* **31**, 4737-4749.

Shih, D. Q., Bussen, M., Sehayek, E., Ananthanarayanan, M., Shneider, B. L., Suchy, F. J., Shefer, S., Bollileni, J. S., Gonzalez, F. J., Breslow, J. L. et al. (2001). Hepatocyte nuclear factor-1alpha is an essential regulator of bile acid and plasma cholesterol metabolism. *Nat. Genet.* **27**, 375-382.

Shiojiri, N. (1997). Development and differentiation of bile ducts in the mammalian liver. *Microsc. Res. Tech.* **39**, 328-335.

Song, Y. H., Ray, K., Liebhaber, S. A. and Cooke, N. E. (1998). Vitamin D-binding protein gene transcription is regulated by the relative abundance of hepatocyte nuclear factors 1alpha and 1beta. *J. Biol. Chem.* **273**, 28408-28418.

Soriano, P. (1999). Generalized lacZ expression with the ROSA26 Cre reporter strain. *Nat. Genet.* **21**, 70-71.

Trauner, M., Meier, P. J. and Boyer, J. L. (1998). Molecular pathogenesis of cholestasis. *New Engl. J. Med.* **339**, 1217-1227.

Tybulewicz, V. L., Crawford, C. E., Jackson, P. K., Bronson, R. T. and Mulligan, R. C. (1991). Neonatal lethality and lymphopenia in mice with a homozygous disruption of the c-abl proto-oncogene. *Cell* **65**, 1153-1163.

van Eyken, P., Sciot, R., van Damme, B., de Wolf-Peeters, C. and Desmet, V. J. (1987). Keratin immunohistochemistry in normal human liver. Cytokeratin pattern of hepatocytes, bile ducts and acinar gradient. *Virchows Arch A Pathol. Anat. Histopathol.* **412**, 63-72.